

## Electrical and environmental parameters of the performance of polymer solar cells based on P3HT:PCBM

El Hadi Chahid<sup>1</sup>, Mohamed Lotfi<sup>2</sup>, Osama Lotfi<sup>3</sup>, My Abdelaziz Koumina<sup>4</sup>, Rodolphe Heyd<sup>5</sup>,  
Abdessamad Malaoui<sup>6</sup>

<sup>1,6</sup>Equipe de Recherche en Electronique, Instrumentation et Mesures, Faculté Polydisciplinaire, Université Sultan Moulay Slimane, Beni Mellal, Morocco

<sup>2,4</sup>Laboratoire Interdisciplinaire de Recherche en Bio-Ressources, Environnement et Matériaux, Ecole Normale Supérieure, Marrakech, Morocco

<sup>2</sup>Laboratoire Matériaux Energie Environnement, Faculté des Sciences Semlalia, Marrakech, Morocco

<sup>3</sup>RES SARL, Beni Mellal, Morocco

<sup>5</sup>Laboratoire Angevin de Mécanique, Procédés et innovAtion (LAMPA), Arts et Métiers ParisTech, Angers, France

### Article Info

#### Article history:

Received Nov 16, 2020

Revised Apr 26, 2021

Accepted Jul 16, 2021

#### Keywords:

Band gap

Efficiency

Photocurrent

Polymer

Solar cell

### ABSTRACT

The electrical and environmental parameters of polymer solar cells (PSC) provide important information on their performance. In the present article we study the influence of temperature on the voltage-current (I-V) characteristic at different temperatures from 10 °C to 90 °C, and important parameters like bandgap energy  $E_g$ , and the energy conversion efficiency  $\eta$ . The one-diode electrical model, normally used for semiconductor cells, has been tested and validated for the polemeral junction. The PSC used in our study are formed by the poly(3-hexylthiophene) (P3HT) and [6,6]-phenyl C61-butyric acid methyl ester (PCBM). Our technique is based on the combination of two steps; the first use the Least Mean Squares (LMS) method while the second use the Newton-Raphson algorithm. The found results are compared to other recently published works, they show that the developed approach is very accurate. This precision is proved by the minimal values of statistical errors (RMSE) and the good agreement between both the experimental data and the I-V simulated curves. The obtained results show a clear and a monotonic dependence of the cell efficiency on the studied parameters.

*This is an open access article under the [CC BY-SA](https://creativecommons.org/licenses/by-sa/4.0/) license.*



### Corresponding Author :

El Hadi Chahid

Equipe de Recherche en Electronique, Instrumentation et Mesures (E.R.E.I.M)

Faculté Polydisciplinaire, Université Sultan Moulay Slimane

Beni Mellal, Morocco

Email: chahid2016@yahoo.com

## 1. INTRODUCTION

Currently, a continuous growing demand for clean sustainable energy has pushed academic as well as industrial institutions to gain a deep understanding of solar cells. Much of today's research focuses on the cells development, material selection and manufacturing with the aim to enhance performance and reduce cost. The current conventional photovoltaic is crystalline silicon known for its non-toxicity, abundance, high and stable cell efficiencies. It has been dominating the solar panels market due to its nature material technology and widespread knowledge, skills and infrastructure for manufacturing and assembly lines. The upper limit of crystalline silicon solar cells efficiency is reaching 26.7% [1]. However, they have lower energy conversion efficiency which make them less space efficient, limited flexibility and cannot be

manufactured in large scale. These limitations of silicon solar cells are some of the reasons that has led many researchers to explore other alternative materials to overcome these issues.

Photovoltaic cells formed by organic polymers or organic molecules are solar cells potentially able to increase the energy efficiency compared to the first and second generations. They are well known for their lightweight, flexibility and low cost to fabricate where the manufacturing techniques vary from coating, spraying and printing [2]. On the contrary, the main disadvantages associated with PSC when compared to inorganic solar cells have low stability in the face of climatic variations and also a low energy efficiency. However, these factors had made the organic solar cells a challenging and popular field of research. The PSCs were able to achieve the highest efficiency of 2.5% as reported in [3], and continues to improve to a record level of 17.35% as presented in solar cell efficiency tables [1], [4]. One of the major obstacles that limit the energy conversion efficiency of organic solar cells lies in the intrinsic properties of the currently used active materials such as, conjugated polymers, preparation and control of their structure (distribution of different lengths of polymer chains in the material). In addition, the PSC tends to suffer from degradation when exposed to harsh ambient conditions (temperature, humidity and rain) as the solar cells are sensitive to high temperature [5], [6]. Several research groups are actively working to address these issues. For instance, a study to investigate the effect of intrinsic parameters which are influenced on the organic cells performance, such as  $V_{oc}$  (open circuit voltage),  $I_{sc}$  (short circuit current) and  $\eta$  (power conversion efficiency) was reported in [7]. Numerous models were also developed to represent the solar cell covering mainly the number of diodes, the shunt resistor and ideality factor. For example, the single diode model M1DR in [8] and two diodes model M2DR in [9]. We consider in the single diode model the following five parameters: the photocurrent  $I_{ph}$ , the reverse saturation current  $I_0$ , the series resistance  $R_s$ , the shunt resistance  $R_{sh}$ , and the diode ideality factor  $n$  [10], [11]. The second problem is focused on the temperature effect of the (I-V) characteristic solar cell. This dependence is described by the sensitivity of the different electrical parameters of the organic photovoltaic generator ( $V_{oc}$ ,  $I_{sc}$ ,  $\eta$ , and  $P_{max}$ ) when the temperature varies. Indeed, the variation of the short circuit current in a remarkable manner, however the open circuit voltage is insensitive to the variation of the temperature [12]-[16]. In literature, several numerical methods were developed for extracting electrical parameters solar cells, such as the least square method, the Newton's method, and the Levenberg Marquardt's method [17]-[20]. As is justified in the literature, an accurate optimization method for parameters extracting is based on the minimization of root mean square error (RMSE) between the theoretical and experimental values to verify the effectiveness of the proposed model [21], [22].

The aim of the current study is to investigate the effect of temperature on the electrical parameters of the polymer solar cells (PSCs) based on poly (3-hexylthiophene) (P3HT) and [6,6]-phenyl C61-butyric acid methyl ester (PCBM). To further enhance the energy conversion efficiency, a developed model of the PSC device using single diode will be presented together with the proposed numerical optimization based on the combination of both the Least Square Method (LMS) and the Newton-Raphson (N-R) Algorithm.

## 2. STRUCTURE AND OPERATION OF POLYMER SOLAR CELL

The general structure of PSC device consists of a transparent substrate such as (glass, quartz, plastic), coated with an electrode, indium tin oxide (ITO), which should be transparent in order to allow the incoming photons to reach the photoactive layer. In addition, a bi-layer of two organic components, with one as the electron donor and the other as the electron acceptor, and finally one top metal electrode, as seen in Figure 1. This bilayer of PSC is the photoactive layer which composes of donor layer and acceptor layer.

A schematic of the basic operation of a PSC is illustrated in Figure 2. the four main steps to produce electrical energy from solar energy by the solar cell are summarized as: i) creation of electron-hole pairs so-called excitons by photons; ii) the excitons formed diffuse towards the donor-acceptor interface (D/A); iii) the minority charge carriers which are the holes in the donor region and the electrons in the acceptor region, move to the contacts for collection due to the internal electric potential/field in the junction; and iv) collecting The charge carriers associate at the electrodes and thus create an electric current.

Figure 3 shows the operation mechanism in P3HT/PCBM cell. The exciton formed is generated, when the incident photon has energy greater than the bandgap energy  $E_g$  of the P3HT. Thus, an electron in the highest occupied molecular orbit (HOMO) would be excited to the lowest unoccupied molecules orbital (LUMO), leaving a hole HOMO band. On the other hand, an efficient solar cell should have a wide absorption spectrum, to create as many pairs as possible of excitons charges due to the Shockley and Queisser limitation [22].

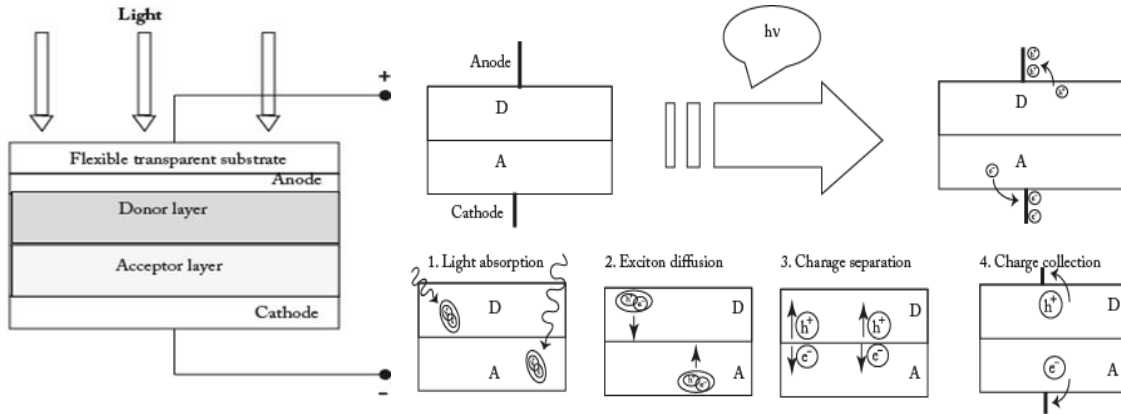


Figure 1. structure of a bilayer polymer solar cell device

Figure 2. Operation mechanism of a bilayer polymer solar cell device (D=donor, A= acceptor)

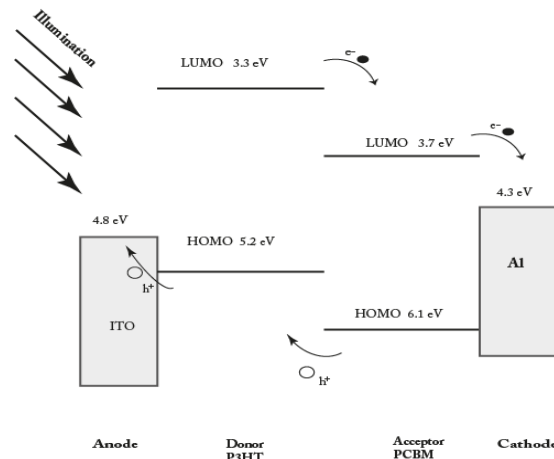


Figure 3. A general operation mechanism in a bilayer P3HT: PCBM cell

The created excitons can be separated if they encounter an internal electric field in the junction. Electrons move from LUMO donor to LUMO acceptor while the holes located in the HOMO acceptor and flows to HOMO donor. However, the diffusion length of charge carriers which is very short makes this process inefficient. Furthermore, the generated charge would be collected at electrodes and more efficient charge collection by utilizing metal oxide-organic interface to decrease surface resistivity and metal oxide-organic to facilitate hole-extraction [23]-[25]. This transfer of carrier charges within the heterojunction, formed by the donor and acceptor of organic semiconductor D/A can produce an open circuit voltage  $V_{oc}$  which is defined as reported in [26]:

$$qV_{oc} = E_{HOMO}^D - E_{LUMO}^A - E_{ex} \tag{1}$$

Where,  $E_{HOMO}^D$  and  $E_{LUMO}^A$  are the acceptor energy LUMO and the donor energy HOMO respectively,  $E_{ex}$  is the exciton binding energy, and  $q$  is the elementary electric charge.

### 3. MODELING OF PSC

The one diode model of polymer solar cell under illumination and the equivalent circuit model is illustrated in Figure 4. The equation of current  $I$  as a function of voltage  $V$  is written as [20]:

$$I(V) = I_{ph} - I_0 \left[ e^{\frac{q(V+IR_s)}{nkT}} - 1 \right] - \frac{V+IR_s}{R_{sh}} \tag{2}$$

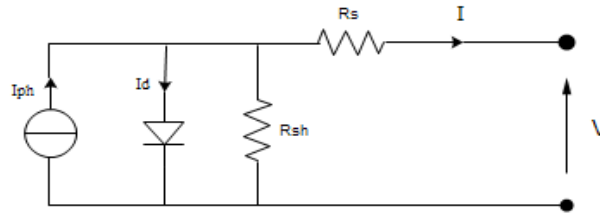


Figure 4. Equivalent circuit model of a polymer solar cell

Where,  $I_{ph}$  and  $I_0$  are the photocurrent and reverse saturation current, the series and parallel resistances are noted as  $R_s$  and  $R_{sh}$ , the ideal factor symbol is noted  $n$ , the Boltzmann's constant is noted  $k$ , and the temperature cell is noted  $T$  and expressed by  $(K)$ .

The photocurrent generated by the cell varies linearly on solar irradiation and is also influenced by the temperature according to the (3) [27]-[29]:

$$I_{ph} = \left( I_{ph,ref} + \lambda_{sc}(T - T_{ref}) \right) \left( \frac{G}{G_{ref}} \right) \quad (3)$$

Where,  $I_{ph,ref}$  is the photocurrent of the module at Standard Test Conditions (STC) (usually  $25^\circ C$  and  $1000W/m^2$ ),  $T_{ref}$  is the reference temperature of the PSC which is given on the data sheet,  $\lambda_{sc}$  is the temperature coefficient of short current which is found on the data sheet and is expressed by  $(A/K)$ ,  $G$  is the irradiation on the device surface (in  $W/m^2$ ), and  $G_{ref}$  is the reference irradiation. The relationship between  $I_0$  as a function of the temperature  $T$  is given by the empirical by Green [30]:

$$I_0 = A \exp - \left( \frac{qE_g}{kT} \right) \quad (4)$$

Where  $A$  is a constant equal to  $1,5 \times 10^8 mA \cdot cm^{-2}$  and  $E_g$  represents the band gap energy. The expression of external quantum efficiency (EQE) is the ration between the electrical energy and the incident photon flux. Then, the EQE is given by [31], [32]:

$$EQE(\%) = 1240 \times \frac{J_{sc}(\lambda)}{\lambda \times \phi_\lambda(T)} \times 100 \quad (5)$$

Where,  $\phi_\lambda(T)$  is the monochromatic light intensity ( $mW/cm^2$ ).  $J_{sc}(\lambda)$  is the photocurrent density ( $mA/cm^2$ ),  $\lambda$  is monochromatic wavelength of light ( $nm$ ). The EQE equal to unit if all photons are observed by the semiconductor. The expression of incident photon flux which depends especially with the body's temperature  $T(K)$  is given by Planck's law [33], [34]:

$$\phi_\lambda(T) = \frac{2\pi hc^2}{\lambda^5} \frac{1}{e^{hc/\lambda k_B T} - 1} \quad (6)$$

Where,  $h$  is the Planck's constant,  $k_B$  is the Boltzmann's constant, and  $c$  is the speed of light in vacuum,  $T$  is the temperature of the black body. The used Planck's law is implemented in a MATLAB script which yields the photon flux of the black body, and it is represented in Figure 5.

On the other hand, the generated current density  $J_{sc}$ , by the PSC with incoming solar radiation, can be calculated from the external quantum efficiency  $EQE(\lambda, T)$ . This evaluation is obtained by integrating over the entire solar radiation spectrum [35]:

$$J_{sc} = q \int_{\lambda_{min}}^{\lambda_{max}} EQE(\lambda) \phi_\lambda(T) d\lambda \quad (7)$$

Where,  $\phi_\lambda(T)$  is the photon flux of solar radiation spectrum under AM<sub>1.5</sub>. Then, the short circuit current can be deduced using the area of the illuminated dvice noted  $A$ . It s written as:  $I_{sc} = A \times J_{sc}$ .

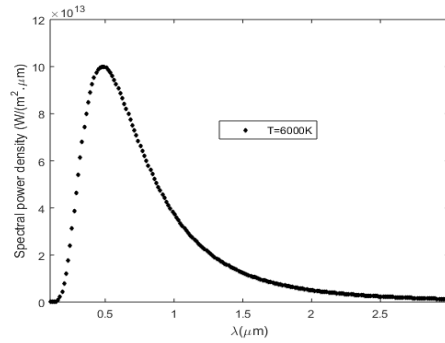


Figure 5. The incident photon flux for an AM<sub>1.5</sub> solar radiation spectrum at 6000 K

#### 4. ELECTRICAL PARAMETERS OF AN PSC

The most important parameter of a PSC is the power conversion efficiency ( $\eta$ ), which represents the ability of the cell to convert light into electricity. It is defined as the ratio between the maximum power output  $P_{max}$  and the incident power  $P_{inc} = 100 \text{ W/m}^2$  at (STC). It is written as:

$$\eta = \frac{P_{max}}{P_{inc}} \times 100\% = \frac{FF \times V_{oc} \times I_{sc}}{P_{inc}} \times 100 \quad (8)$$

Where  $FF$  is the Fill Factor corresponding to the maximum power ratio on the ideal theoretical power.  $FF$  describes the part of energy loss in the form of Joule heat, which mainly determined by surface resistivity and it expressed as:

$$FF = \frac{P_{max}}{V_{oc} \times I_{sc}} \times 100\% = \frac{V_{max} \times I_{max}}{V_{oc} \times I_{sc}} \times 100\% \quad (9)$$

The short circuit current  $I_{sc}$  is the current when the voltage across the device is zero, and the open-circuit voltage  $V_{oc}$  is the voltage when the current in the device is zero. According to the (9) and (10), it is clear that a high efficiency could be reached with higher  $V_{oc}$ ,  $I_{sc}$  and  $FF$ . The voltage  $V_{oc}$  can be expressed as a function of the currents  $I_{sc}$  and  $I_0$ . It can be written as [30]:

$$V_{oc} = \frac{nkT}{q} \ln \left( \frac{I_{sc}}{I_0} - 1 \right) \quad (10)$$

#### 5. DEVELOPED METHOD OF EXTRACTING ELECTRICAL PARAMETERS

Determining the final optimal parameters values requires first an estimation of the initial guess assigned to the extracted parameters  $\theta_0 [I_{ph}, I_0, R_s, R_{sh}, n]$ ; which affect the convergence of the Newton-Raphson's algorithm (N-R). The initial parameters  $\theta_0$  are obtained from the current-voltage experimental curve using the least mean square (LMS) method. This technique is one of the most widely used methods for modeling experimental measurements by a predetermined analytical function given by (2). This method consists to minimize the mean absolute or relative difference between the  $N$  measures  $I_m (V_i)$  and the calculated values of electric current  $I_c (V_i)$  obtained by (2). The mathematical model of single diode for estimation five parameters in the form as:

$$f(I_i, V_i, \theta) = I_{ph} - I_0 \left[ e^{\frac{q(V+IR_s)}{nkT}} - 1 \right] - \frac{V+IR_s}{R_{sh}} - I \quad (11)$$

The second step, we use the N-R algorithm to determine the final five unknown electrical parameters  $\theta [I_{ph}, I_0, R_s, R_{sh}, n]$  which characterize the single diode model of the polymer solar cell. The N-R method is widely used in finding the root of nonlinear equations. This method uses the derivative of  $f(x)$  at  $x$  to estimate a new value of the root. The desired precision is reached by iteration. if  $\theta_{i+1}$  is an approximation to the root of  $f(\theta) = 0$ . The N-R is an iterative method that estimate the root of a real valued nonlinear function  $f(\theta)$  with an initial guess  $\theta_0$ . This linearization process is obtained through the first order Taylor's series expansion (linear in  $\theta$ ) to the first around the guess ( $\theta_i$ ), which is given below [36]:

$$f(\theta_{i+1}) = f(\theta_i) + (\theta_{i+1} - \theta_i)f'(\theta_i) + \dots = 0 \tag{12}$$

Therefore, the next approximation to the root  $\theta_i$  in the  $i$ th iterative step is given by the iterative formula [37]:

$$\theta_{i+1} = \theta_i - f(\theta_i)/f'(\theta_i) \tag{13}$$

The procedure is repeated until  $|\theta_{i+1} - \theta_i| < \varepsilon$ , where  $\varepsilon$  is a preset tolerance. The N-R method is easily extended to the solution of set of  $n$ -nonlinear equations, where  $n \geq 2$ . Therefore, the parameters  $\theta$  are evaluated at each iteration according to the formula [21]:

$$\theta_i = \theta_{i-1} - [J(\theta)]_{\theta_{i-1}}^{-1} \times [f]_{\theta_{i-1}} \tag{14}$$

Where  $J$  is the Jacobian matrix for the function  $f(\theta)$  given by the first-order contains the partial derivatives at each parameter of the vector  $\theta_i$ . It is defined by:  $J_{ij} = \frac{\partial f_i}{\partial \theta_j}$ ,  $\Delta\theta = \theta_i - \theta_{i-1}$  denotes the change in the value of the vector of roots (step size). The used function  $\varphi$  to optimize the electrical parameters is the objective function  $\varphi$ , which is defined as the difference between both of the experimental  $I^{exp}$  and calculated  $I^{cal}$  electric current values. The expression of  $\varphi$  can be given by:

$$\varphi(I_i, V_i, \theta) = \sum_{i=1}^N (I_i^{exp} - I_i^{the})^2 = \sum_{i=1}^N e_i^2(\theta_i) \tag{15}$$

Where,  $e_i = I_i^{exp} - I_i^{cal}$ , is the error between the experimental and theoretical electric currents  $I_i^{exp}$  and  $I_i^{cal}$  respectively, and  $N$  is the number of measurements. To validate our adopted method and evaluates its degree of precision, we use the root mean square error (RMSE) which is written as:

$$RMSE = \sqrt{\frac{1}{N} \sum_{i=1}^N (e(I_i, V_i, \theta_i))^2} \tag{16}$$

Where  $(I_i, V_i)$  represents the  $i$ th measured value of  $N$  experimental data. In a MATLAB script, the flowchart of the developed method is shown in Figure 6.

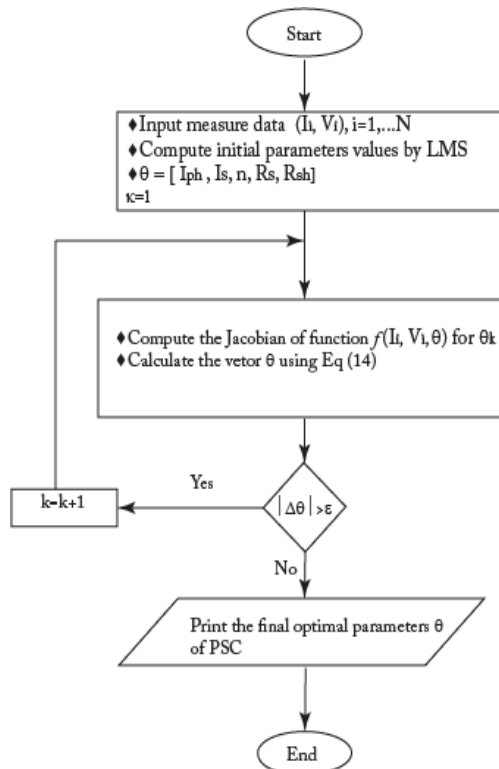


Figure 6. Flowchart for estimation PSCs parameters using the developed method

## 6. RESULTS AND DISCUSSION

In this section, we will present the results of the theoretical research related to the dependence of the PSCs energy conversion efficiency with the temperature and the intrinsic electrical parameters by using the single diode model. The simulated results of  $I$ - $V$  characteristic, under the Standard Test Conditions ( $STC$ ) at  $AM_{1.5}$ , were carried out using the developed method which is composed of two means. The first one is the least mean square method (LMS) so as to determine the initial electrical parameters  $\theta_0 [I_{ph}, I_0, R_s, R_{sh}, n]$ , and the second one is the Newton- Raphson's algorithm (N-R) to evaluate the final optimal values.

Figure 7 shows both the calculated and experimental curves of the P3HT: PCBM polymer solar cell. That is, the experimental curve was represented by the squares in the Figure 7, whose the data points  $(I_i, V_i)$  with  $(i = 1, \dots, 36)$  are from the reference cell [38], what's more, the calculated curve was schematized by the solid line.

As it is shown in Figure 7, there is a very good agreement between the simulation results and the experimental data  $(I_i, V_i)$ . In the developed method, the LMS method is used to determine the initial parameters so as to ensure the convergence of the Newton's algorithm. The final values of the five parameters are substituted in (2), and are obtained while the error criterion  $\Delta\theta = |\theta_{i+1} - \theta_i|$  is minimized. Then the PSC's parameters which are found by the developed method are listed in Table 1 and compared to the references work.

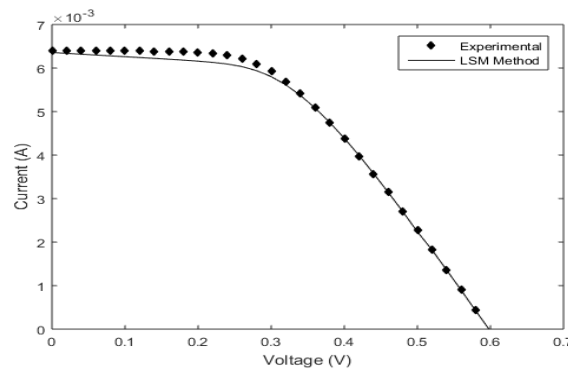


Figure 7. Calculated and experimental I-V characteristics of P3HT: PCBM polymer solar cell

Table 1. Comparison of estimated parameters for single diode model of PSC

Electrical Parameters	Proposed method	Ref[39]	Ref[40]	Ref[41]
$I_{ph}(mA)$	6.59	6.4	6.4	6.4
$I_s(A)$	$1.46 \times 10^{-14}$	$2.00 \times 10^{-08}$	$2.63 \times 10^{-10}$	$2.21 \times 10^{-12}$
$n$	0.84	3.027	1.363	1.068
$R_{sh}(\Omega)$	1038.13	36200	36300	36400
$R_s(\Omega)$	38.85	107.42	35.46	38.24

From the results presented in Table 1, it is clearly seen that the five electrical parameters evaluated by the proposed method are quite closer than those found in the references [39]-[41]. The highest precision of the extracted values is directly attached to the lowest value of the root mean squared error (RMSE), which measures the average of squared differences between prediction and real in a set of electric current values. The found values of the statistical error (RMSE) are presented in Table 2 and compared to the reference values [39]-[41].

Table 2. Statistical error (RMSE)of electrical parameters model

Statistical Error	Proposed Method	Ref[39]	Ref[40]	Ref[41]
RMSE	$1.0012 \times 10^{-4}$	$2.3423 \times 10^{-3}$	$1.4936 \times 10^{-3}$	$6.3944 \times 10^{-4}$

According to the statistical error, the obtained value by the proposed method is lower than those found by other works [39]-[41]. As a result, our proposed method is more accurate than the other methods. In addition, the program's execution is fairly fast than the other programs. In what follows, we will study the

effect of the influence of many factors on the PSC operation, such as: temperature, series and shunt resistances, ideality factor and illumination. This effect will be shown through both the variation of I-V and P-V characteristics in order to optimize the energy conversion efficiency of polymer solar cell.

### 6.1. Temperature cell effect on PSC parameters

The Figure 8 shows the impact of the temperature cell ranging from 10°C to 90°C on the I-V and P-V characteristics of the P3HT: PCBM polymer solar cell. It is observed that the increase of the temperature produces an increase in the short-circuit current ( $I_{sc}$ ) and a decrease in open circuit voltage ( $V_{oc}$ ). On the other hand, the increase in the temperature leads to a decrease in maximum voltage ( $V_m$ ) and a slight increase in maximum current ( $I_m$ ) and consequently a relative decrease in maximum power ( $P_{max}$ ). Figure 8 (a) shows Effect of temperature on the I-V. Figure 8 (b) shows Effect of temperature on the P-V characteristics.

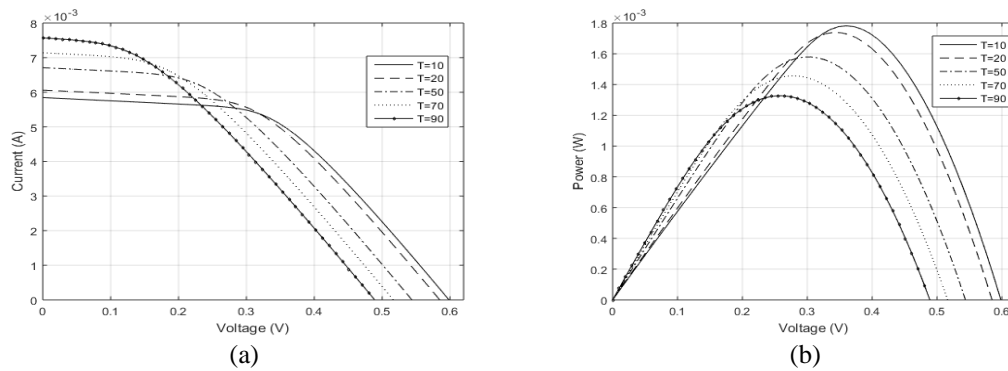


Figure 8. Effect of temperature on the (a) I-V and (b) P-V characteristics

Figure 9 represents the variation of the gap energy and the energy conversion efficiency of PSC as a function of temperature. It is seen that both the cell efficiency  $\eta$ (%) and the bandgap energy  $E_g$  decreases when the temperature  $T$  increases as described by Varshni's empirical expression [42]. Figure 9 (a) shows Efficiency. Figure 9 (b) shows band gap energy of PSC as a function of temperature.

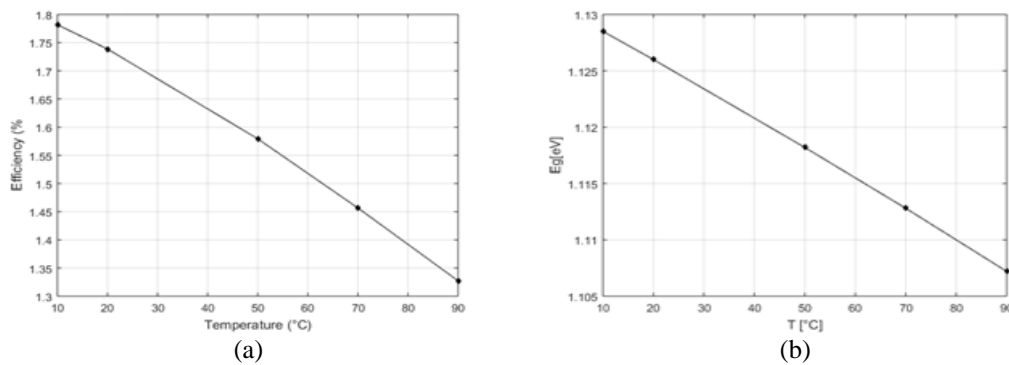


Figure 9. (a) Efficiency and (b) band gap energy of PSC as a function of temperature

$$E_g(T) = E_g(0) - \frac{\alpha T^2}{T + \beta} \quad (17)$$

Where  $E_g(0)$  is the bandgap energy at theoretical zero temperature of material,  $\alpha$  and  $\beta$  are material constants. As a suggestion, to enhance the PSC's performance could be achieved through the choice of new material in the solar cell domain like perovskite material which is a hybrid of organic and inorganic material [43], [44].

### 6.2. Series resistance effect

The effect of the series resistance  $R_s$  on the I-V and P-V curves of the solar cell are illustrated in Figure 10. We remark when the series resistance  $R_s$  increases, the short-circuit current  $I_{sc}$  is reduced but the open-circuit voltage  $V_{oc}$  is not changed. This influence is characterized by a decrease of the slope in the area of high voltages. In fact, the series resistance  $R_s$  characterizes the losses of proper semi-conductor resistance and the electrode-organic solar cell contacts ( $Al/OSC$ ). As an effect, a high of this resistance decrease appreciably the voltage and the output current, and consequently will limit the energy conversion efficiency. Besides, when the resistance arises, we perceive a decrease of the output power of the PSC in a considerable manner. Figure 11 (a) shows Effect of series resistances on the I-V. Figure 13 (b) shows Effect of series resistances on the P-V characteristics

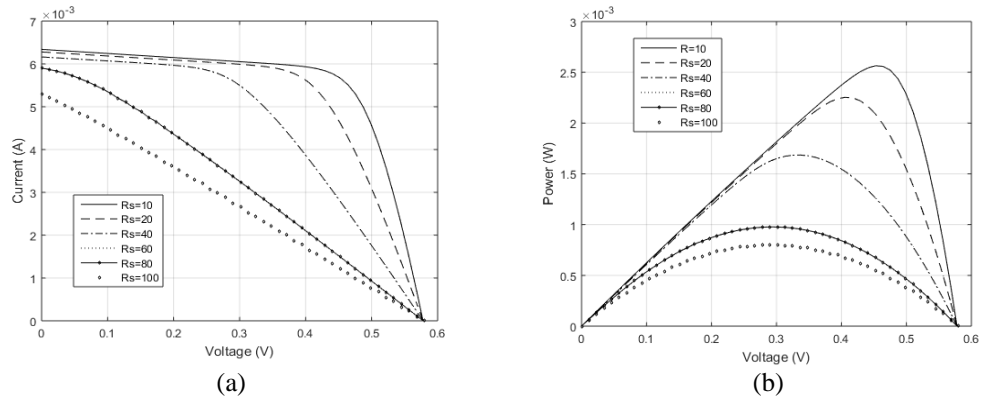


Figure 10. Effect of series resistances on the (a) I-V and (b) P-V characteristics

### 6.3. Shunt resistance effect

These Figure 11 (a) shows illustrates the effect of the shunt resistance  $R_{sh}$  on the I-V. Figure 11 (b) shows Effect of shunt on the P-V characteristics of P3HT: PCBM solar cell. We notice that when  $R_{sh}$  arises, the short-circuit current  $I_{sc}$  decreases while the open-circuit voltage  $V_{oc}$  remain constant; moreover, this influence is characterized by an increase of the slope in the low voltages region. Besides this, the output power increases when  $R_{sh}$  decreases. Indeed, the shunt resistance of the D/A junction causes the leakage phenomenon and then leads to the losing a part of the photocurrent  $I_{ph}$  in the inner of solar cell device. As a result, when the parallel resistance is as high as possible, the maximum power conversion efficiency is decreased.

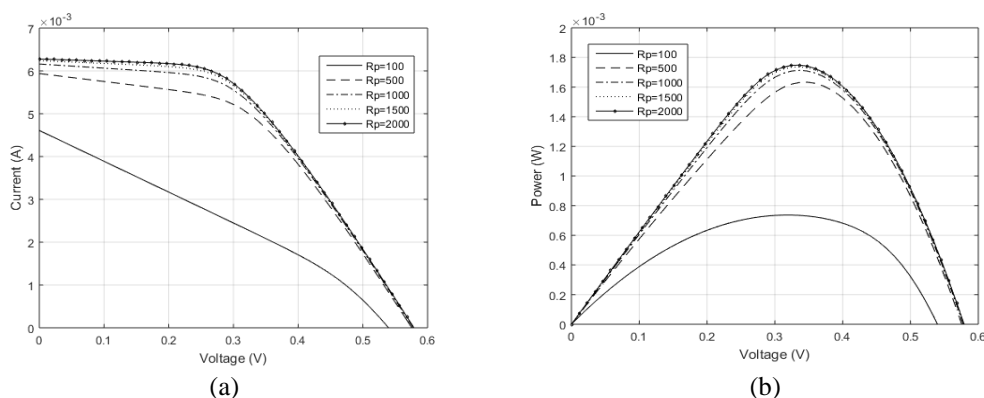


Figure 11. Effect of shunt resistances on the (a) I-V and (b) P-V characteristics

**6.4. Influence of the ideality factor**

These Figure 12 (a) shows the influence of the ideality factor  $n$  on the I-V and Figure 12 (b) shows the influence of the ideality factor  $n$  on the P-V characteristics of the solar cell under the Standard Test Conditions. It can be seen that the decrease of the ideality factor  $n$  causes a reduction in the open circuit voltage  $V_{oc}$ , while the short-circuit current  $I_{sc}$  remains constant.

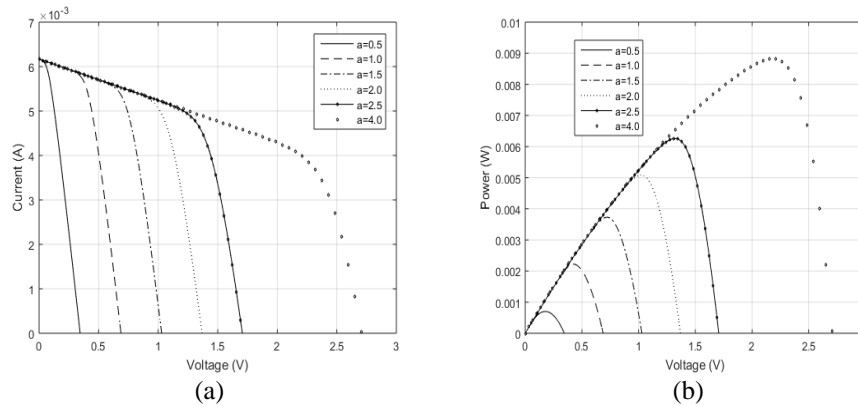


Figure 12. Effect of ideality factor  $n$  on the (a) I-V and (b) P-V characteristics

**6.5. Illumination effect**

Figure 13 represents the current-voltage and power-voltage characteristics of a polymer solar cell for different solar irradiation ranging from  $E = 200 W/m^2$  to  $E = 1400 W/m^2$ . We notice that the short-circuit current  $I_{sc}$  increases significantly comparing to the open circuit voltage  $V_{oc}$ . In fact, the short-circuit current varies linearly as a function of the illumination, whereas the open circuit voltage varies logarithmically [29], [30] as a function of the illumination. As a result, the increase of solar irradiation causes an increase in the maximum voltage  $V_m$ , the maximum current  $I_m$  and subsequently a net increase in the maximum power  $P_{max}$ . Figure 13 (a) shows Effect of illumination on the I-V. Figure 13 (b) shows Effect of illumination on the P-V characteristics.

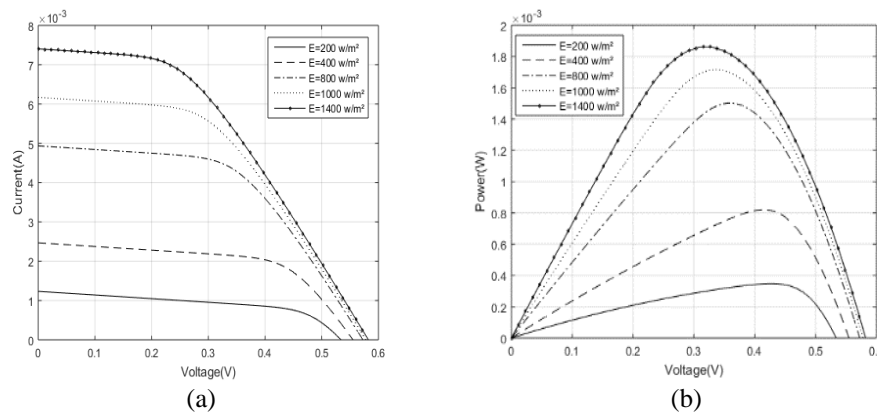


Figure 13. Effect of illumination on the (a) I-V and (b) P-V characteristics

**7. CONCLUSION**

In this paper, we have studied the dependence both of the intrinsic electrical and the external parameters (illumination, temperature, series and parallel resistances, and ideality factor) on the performance of polymer solar cells (PSCs) based on the poly(3-hexylthiophene) (P3HT) and [6,6]-phenyl-C61-butyric acid methyl ester (PCBM). The single diode model is used to represent the PSC, which is identified by the five electrical parameters ( $I_{ph}$ ,  $I_0$ ,  $R_s$ ,  $R_{sh}$ , and  $n$ ). The proposed method performed by the combination of least

mean square method (LMS) and the Newton Raphson's method to determine the final optimal values of the PSC's parameters.

The effect of temperature on both the I-V and P-V characteristics, energy band gap, and the energy conversion efficiency at different temperatures from 10°C and 90°C has studied, and the influence of the electrical and environmental parameters on both of the I-V and P-V characteristic's PSC. The obtained results show that the calculated currents are in a good agreement with the experimental data, and the difference between both of the calculated and the experimental currents does not exceed 10% referring to the RMSE statistical error. Concerning the effect of the temperature, we have found an increase of  $I_{sc}$ , a decrease of  $V_{oc}$  with increasing of the temperature. However, the variation of the intrinsic electrical parameters shows a dependence of the PSC's efficiency, that we can use in the improvement of PSC performance by taking the optimal intrinsic and external parameters.

## REFERENCES

- [1] M. A. Green, E. D. Dunlop, J. Hohl-Ebinger, M. Yoshita, N. Kopidakis, and A. W. Y. Ho-Baillie, "Solar cell efficiency tables (version 55)," *Progress in Photovoltaics: Research and Applications*, vol. 28, no. 1, pp. 3-15, 2020, doi: 10.1002/pp.3228.
- [2] Z. Yin, J. Wei, and Q. Zheng, "Interfacial materials for organic solar cells: recent advances and perspectives," *Advanced Science*, vol. 3, no. 8, pp. 1-37, 2016, doi: 10.1002/advs.201500362.
- [3] S. Shaheen, C. Brabec, N. S. Sariciftci, F. Padinger, T. Fromherz, and J. Hummelen "2.5% efficient organic plastic solar cells," *Applied Physics Letters*, vol. 78, pp.841-843, 2001, doi: 10.1063/1.1345834.
- [4] Z. Li *et al*, "A generic green solvent concept boosting the power conversion efficiency of all-polymer solar cells to 11%," *Energy Environmental Science*, vol. 12, pp. 157-163, 2019, doi: 10.1039/C8EE02863J.
- [5] E. Bundgaard, O. Hagemann, M. Manceau, M. Jorgensen, and F. Krebs, "Low band gap polymers for roll-to-roll coated polymer solar cells," *Macromolecules*, vol. 43, no. 19, pp. 8115-8120, Aug 2010, doi: 10.1021/ma1015903.
- [6] M. Jørgensen, K. Norrman, and F. C. Krebs, "Stability/degradation of polymer solar cells," *Solar Energy Materials and Solar Cells*, vol. 92, no. 7, pp. 686-714, July 2008, doi: 10.1016/j.solmat.2008.01.005.
- [7] D. T. Cofas, P.A. Cofas, and S. Kaplanis, "Methods to determine the parameters of solar cells: a critical review," *Renewable and Sustainable Energy Reviews*, vol. 28, pp. 588-596, 2013, doi: 10.1016/j.rser.2013.08.017.
- [8] E. Chahid, and M. Idali Oumhand. A. Malaoui, "A fast Strategy to determine the physical and electrical parameters of photovoltaic silicon cell," *International Journal of Applied Power Engineering (IJAPE)*, vol. 6, no. 2, pp. 103-112, 2017, doi: 10.11591/ijape.v6.i2.pp103-112.
- [9] A. Malaoui, E. Barah, and J. Antari, "Implementation a new approach for modeling and determining the electrical parameters of solar cells," *International Journal of Innovation and Applied Studies*, vol. 15, no. 2, pp. 329-338, 2016.
- [10] E. Chahid, M. I. Oumhand, M. Feddaoui, M. Erritali, and A. Malaoui, "Effect of measurement factors on photovoltaic cell parameters extracting," *International Journal of Electrical and Computer Engineering (IJECE)*, vol. 7, no.1, pp. 50-57, Feb 2017, doi: 10.11591/ijece.v7i1.pp50-57.
- [11] A. Malaoui, "New method for improving the quality of electrical measurements: application to the extraction of the intrinsic parameters of the photovoltaic cells," *International Journal of Innovation and Applied Studies*, vol. 15, no. 2, pp. 375-386, 2016.
- [12] S. Chander, A. Purohit, A. Sharma, Arvind, S. P. Nehra, and M. S. Dhaka, "A study on photovoltaic parameters of monocrystalline silicon solar cell with cell temperature," *Energy Reports*, vol. 1, pp. 104-109, 2015, doi: 10.1016/j.egy.2015.03.004.
- [13] O. Dupré, R. Vaillon, and M. A. Green, "Experimental assessment of temperature coefficient theories for silicon solar cells," *IEEE Journal of Photovoltaics*, vol. 6, no. 1, pp. 56-60, Jan. 2016, doi: 10.1109/JPHOTOV.2015.2489864.
- [14] P. Singh, and N. M. Ravindra, "Temperature dependence of solar cell performance—an analysis," *Solar Energy Materials and Solar Cells*, vol. 101, pp. 36-45, 2012, doi: 10.1016/j.solmat.2012.02.019.
- [15] A. B. Or, J. Appelbaum, "Dependence of multi-junction solar cells parameters on concentration and temperature," *Solar Energy Materials and Solar Cells*, vol. 130, pp. 234-240, 2014, doi: 10.1016/j.solmat.2014.07.010.
- [16] D. T. Cofas, P. A. Cofas, and O. M. Machidon, "Study of temperature coefficients for parameters of photovoltaic cells," *International Journal of Photoenergy*, vol. 130, pp. 1-12, 2018, doi: 10.1155/2018/5945602.
- [17] W. T. Vetterling, and S. A. Teukolsky, *Numerical recipes in C: the art of scientific computing*, 2nd edition, UK: Cambridge University Press, WH. Press, pp. 1-949, 1992.
- [18] M. K. Gupta, and R. Jain, "Design and simulation of photovoltaic cell using decrement resistance algorithm," *Indian Journal of Science and Technology*, vol. 6, no. 5, pp. 4537-4541, 2013, doi: 10.17485/ijst/2013/v6i5.21.
- [19] D. Marquardt, "An algorithm for least squares estimation of non linear parameters," *Journal of the Society for Industrial and Applied Mathematics*, vol. 11, no. 2, pp. 431-41, 1963.
- [20] K. Bouzidi, M. Chegaar, and A. Bouhemadou, "Solar cells parameters evaluation considering the series and shunt resistance," *Solar Energy Materials & Solar Cells*, vol. 91, no. 18, pp. 1647-1651, 2007, doi: 10.1016/j.solmat.2007.05.019.
- [21] F. Dkhichi, B. Oukarfi, A. Fakkar, and N. Belbounaguia, "Parameter identification of solar cell model using Levenberg-Marquardt algorithm combined with simulated annealing," *Solar Energy*, vol. 110, pp. 781-788, 2014.

- [22] W. Shockley, and H. Queisser, "Detailed balance limit of efficiency of p-n junction solar cells," *Journal of Applied Physics*, vol. 32, no. 3, pp. 510-519, 1961, doi: /10.1016/j.solener.2014.09.033.
- [23] B. Kippelen, and J. Bredas, "Organic photovoltaics," *Energy & Environmental Science*, vol. 2, pp. 251-261, 2009, doi: 10.1039/B812502N.
- [24] L. Hung, C. Tang, and M. Mason, "Enhanced electron injection in organic electroluminescence devices using an Al/LiF electrode," *Applied Physics Letters*, vol. 70, no. 2, pp. 152-154, 1997, doi: 10.1063/1.118344.
- [25] R. A. Hatton, N. P. Blanchard, L. W. Tan, G. Latini, F. Cacialli, and S. R. Silva, "Oxidised carbon nanotubes as solution processable, high work function hole-extraction layers for organic solar cells," *Organic Electronics*, vol. 10, no. 3, pp. 388-395, 2009, doi: 10.1016/j.orgel.2008.12.013.
- [26] J. Crispim, M. Carreira, and R. Castro, "Validation of photovoltaic electrical models against manufacturers data and experimental results," in *2007 International Conference on Power Engineering, Energy and Electrical Drives*, 2007, pp. 556-561, doi: 10.1109/POWERENG.2007.4380161.
- [27] D. Sera, R. Teodorescu, and P. Rodriguez, "PV panel model based on datasheet values," in *2007 IEEE International Symposium on Industrial Electronics*, 2007, pp. 2392-2396, doi: 10.1109/ISIE.2007.4374981.
- [28] W. De Soto, S. A. Klein, and W. A. Beckman, "Improvement and validation of a model for photovoltaic array performance," *Solar Energy*, vol. 80, no. 1, pp. 78-88, 2006, doi: 10.1016/j.solener.2005.06.010.
- [29] A. Driesse, S. Harrison, and P. Jain, "Evaluating the effectiveness of maximum power point tracking methods in photovoltaic power systems using array performance models," in *2007 IEEE Power Electronics Specialists Conference*, 2007, pp. 145-151, doi: 10.1109/PESC.2007.4341978.
- [30] M. A. Green, *Solar cells: Operating principles, technology and system applications*, Englewood Cliffs, NJ, Prentice-Hall, Inc., 1982.
- [31] S. Dhar, T. Majumder, and S. P. Mondal, "Graphene quantum dot-sensitized ZnO nanorod/polymer schottky junction UV detector with superior external quantum efficiency, detectivity, and responsivity," *ACS Applied Materials & Interfaces*, vol. 8, no. 46, pp. 31822-31831, 2016, doi: 10.1021/acsami.6b09766.
- [32] J. J. L. Hmar, T. Majumder, S. Dhar, and S. P. Mondal, "Sulfur and Nitrogen Co-doped graphene quantum dot decorated ZnO nanorod/polymer hybrid flexible device for photosensing applications," *Thin Solid Films*, vol. 612, pp. 274-283, 2016, doi: 10.1016/j.tsf.2016.06.014.
- [33] R. Shankar, *Principles of quantum mechanics*, 2nd ed., Springer, New York, 1994.
- [34] T. Fukushima, "Precise and fast computation of Lambert W-functions without transcendental function evaluations," *Journal of Computational and Applied Mathematics*, vol. 244, pp.77-89, 2013, doi: 10.1016/j.cam.2012.11.021.
- [35] H. Zhao, "Light trapping for silicon solar cells: theory and experiment," ph.D. dissertations, Dept of Physics, Syracuse University, 2013.
- [36] M. D. Smith, "Newton-Raphson technique," 1998, Electronic document [Online] Available: [http://web.mit.edu/10.001/Web/Course\\_Notes/NLAE/node6.html](http://web.mit.edu/10.001/Web/Course_Notes/NLAE/node6.html). Accessed in October, 02, 2016.
- [37] A. Ben-Israel, "A Newton-Raphson method for the solution of systems of equations," *Journal of Mathematical Analysis and Applications*, vol. 15, no. 2, pp. 243-252, 1966, doi: 10.1016/0022-247X(66)90115-6.
- [38] G. Williams, *Advances in organic photovoltaics and methods for effective solar cell parameter extraction*, University of Waterloo. Waterloo, On Canada. N2L 3G1, 2016.
- [39] N. Nehaoua, Y. Chergui, and D. E Mekki, "Determination of organic solar cell parameters based on single or multiple pin structures," *Vacuum*, vol. 84, no. 2, pp. 326-329, 2009, doi: 10.1016/j.vacuum.2009.07.006.
- [40] M. Chegaar, G. Azzouhi, and P. Mialhe, "Simple parameter extraction method for illuminated solar cells," *Solid State Electronics*, vol. 50, no. 7-8, pp. 1234-1237, 2006, doi: 10.1016/j.sse.2006.05.020.
- [41] A. Jain, and A. Kapoor, "A new method to determine the diode ideality factor of real solar cell using Lambert W-function," *Solar Energy Materials and Solar Cells*, vol. 85, no. 3, pp. 391-396, 2005, doi: 10.1016/j.solmat.2004.05.022.
- [42] Y. P. Varshni, "Temperature dependence of the energy gap in semiconductors," *Physica*, vol. 34, no. 1, pp. 149-154, 1967, doi: 10.1016/0031-8914(67)90062-6.
- [43] P. Tonui, S. O. Osenia, G. Sharmab, Q. Yanc, and G. T. Mola, "Perovskites photovoltaic solar cells: An overview of current status," *Renewable and Sustainable Energy Reviews*, vol. 91, pp. 1025-1044, 2018, doi: 10.1016/j.rser.2018.04.069.
- [44] M. A. Green, and A. Ho-Baillie, "Perovskite solar cells: the birth of a new era in photovoltaics," *ACS Energy Letters*, vol. 2, no. 4, pp. 822-830, 2017, doi: 10.1021/acsenergylett.7b00137.